

This article was downloaded by:

On: 23 January 2011

Access details: *Access Details: Free Access*

Publisher *Taylor & Francis*

Informa Ltd Registered in England and Wales Registered Number: 1072954 Registered office: Mortimer House, 37-41 Mortimer Street, London W1T 3JH, UK



Journal of Coordination Chemistry

Publication details, including instructions for authors and subscription information:

<http://www.informaworld.com/smpp/title~content=t713455674>

Synthesis and X-Ray Molecular Structure Analysis of Tricobalt Clusters With Multi Ferrocenyl Groups

Satoru Onaka^a; Yoshitaka Katsukawa^a; Hitoshi Muto^a

^a Department of Environmental Technology, Graduate School of Engineering, Nagoya Institute of Technology, Nagoya, Japan

To cite this Article Onaka, Satoru , Katsukawa, Yoshitaka and Muto, Hitoshi(2008) 'Synthesis and X-Ray Molecular Structure Analysis of Tricobalt Clusters With Multi Ferrocenyl Groups', Journal of Coordination Chemistry, 51: 1, 33 – 44

To link to this Article: DOI: 10.1080/00958970008047076

URL: <http://dx.doi.org/10.1080/00958970008047076>

PLEASE SCROLL DOWN FOR ARTICLE

Full terms and conditions of use: <http://www.informaworld.com/terms-and-conditions-of-access.pdf>

This article may be used for research, teaching and private study purposes. Any substantial or systematic reproduction, re-distribution, re-selling, loan or sub-licensing, systematic supply or distribution in any form to anyone is expressly forbidden.

The publisher does not give any warranty express or implied or make any representation that the contents will be complete or accurate or up to date. The accuracy of any instructions, formulae and drug doses should be independently verified with primary sources. The publisher shall not be liable for any loss, actions, claims, proceedings, demand or costs or damages whatsoever or howsoever caused arising directly or indirectly in connection with or arising out of the use of this material.

SYNTHESIS AND X-RAY MOLECULAR STRUCTURE ANALYSIS OF TRICOBALT CLUSTERS WITH MULTI FERROCENYL GROUPS

SATORU ONAKA*, YOSHITAKA KATSUKAWA
and HITOSHI MUTO

*Department of Environmental Technology, Graduate School of Engineering,
Nagoya Institute of Technology, Gokiso-cho, Showa-ku, Nagoya 466-8555, Japan*

(Received 16 March 1999; Revised 8 June 1999; In final form 11 November 1999)

The reaction of $\text{NaCo}(\text{CO})_4$ with "impure FcPcCl_2 " in THF afforded two dark green products in low yield after column chromatography on silica-gel. Single crystal X-ray analysis showed that the products are $\text{Co}_3(\text{CO})_7(\mu_3\text{-Pfc})(\mu_2\text{-Pfc}_2)$ (1) and $\text{Co}_3(\text{CO})_7(\mu_3\text{-Pfc})(\mu_2\text{-P(H)Fc})$ (2). Both clusters have a tetrahedral skeleton composed of a capping $\mu_3\text{-Pfc}$, a basal Co_3 triangle, and an edge (the Co–Co bond) bridging $\mu_2\text{-P(R)Fc}$ group. Both clusters have 48 total skeletal electrons. The Co–Co bond to which the $\mu_2\text{-P(R)Fc}$ group bridges is significantly shorter than the other Co–Co bonds, but these are in the range of single Co–Co bonds. CV measurements have shown that two reduction peaks are observed for 1 while a single reduction peak is observed for 2.

Keywords: Cobalt cluster; multiferrocenyl groups; X-ray structure;
total skeletal electron; CV

INTRODUCTION

In a previous communication, we described the unexpected isolation of a tricobalt cluster with three ferrocenyl groups, $\text{Co}_3(\text{CO})_7(\mu_3\text{-Pfc})(\mu_2\text{-Pfc}_2)$ (1) from the reaction of $\text{FcPcCl}_2(\text{Fc} = (\text{C}_5\text{H}_5)\text{Fe}(\text{C}_5\text{H}_4))$ with $\text{NaCo}(\text{CO})_4$

* Corresponding author. E-mail: onklustr@ks.kyy.nitech.ac.jp.

in THF at room temperature.¹ We suggested that a small amount of impurities such as Fc_2PCL contained in “ FcPCL_2 ” was responsible for the formation of this cluster. If this suggestion is true, it is anticipated that other clusters should be formed during the reaction; therefore, we have explored the reaction of “impure FcPCL_2 ” with $\text{NaCo}(\text{CO})_4$ and have carried out column chromatography carefully. We have found that a new cluster $\text{Co}_3(\text{CO})_7(\mu_3\text{-PFc})(\mu_2\text{-P(H)Fc})$ (**2**) is obtained in addition to **1** with significant improvement of the yield of **1** when “impure FcPCL_2 ” is used. We describe the detailed synthetic procedures and results on single crystal X-ray analysis for these trinuclear clusters.

EXPERIMENTAL

Materials and General Procedures

Synthesis and manipulations were made under an argon atmosphere with standard Schlenk-line techniques. Solvents were purified by standard procedures before use. FcPCL_2 was synthesized by literature method² with slight modifications: (1) *in situ* prepared Et_2NPCl_2 was used instead of Me_2NPCl_2 , (2) the refluxing time of the mixture of Et_2NPCl_2 , ferrocene, and AlCl_3 was prolonged to 20 h, and (3) the resulting “ FcPCL_2 ” was extracted with dichloromethane instead of heptane to make it possible to dissolve impurities other than FcPCL_2 . IR spectra were obtained by use of a JASCO Valor-III FT-IR spectrometer. ³¹P-NMR spectra were recorded on a Varian XL-200 spectrometer operated at 80.984 MHz with Fourier transform mode and referenced to external H_3PO_4 .

Synthesis of $\text{Co}_3(\text{CO})_7(\mu_3\text{-PFc})(\mu_2\text{-P(H)Fc})$ (**2**)

A THF solution (30 mL) in which “ FcPCL_2 ” (3.4 mmol, 1.0 g) was dissolved was slowly added to an ice-cooled THF solution (30 mL) of $\text{NaCo}(\text{CO})_4$ prepared from 1.36 g of $\text{Co}_2(\text{CO})_8$ (4.0 mmol) stirred over sodium amalgam. Vigorous gas evolution was observed. The mixture was stirred in an ice-cooled bath for several hours; then gradually warmed to room temperature for 20 h with stirring. The solvent was vacuum-stripped from the resulting red-brown solution to leave a green-brown oil. The oil was dissolved in a minimum amount of benzene and the solution was loaded on a Yamazen YFLC-700 medium-pressure liquid chromatography instrument (Wako-gel C-200). After the first huge red band and then an orange band were eluted

with hexane:benzene (1:4), a dark green band was eluted with the same mixed solvent. After the solvent was distilled off, the dark green residue was subjected to a TLC (silica-gel) test which showed the existence of two green components. The dark green residue was then dissolved into a minimum amount of benzene and the solution was loaded on the same medium-pressure liquid chromatograph with a longer column (50 cm) packed with Wako-gel C-200. Two components were eluted with a mixed solvent of benzene-hexane (1:4). The first dark green product was recrystallized from hexane to afford **2** and **1** was obtained from the second green band. The yield of the crude product is approximately 60 mg for **1** and approximately 30 mg for **2**, respectively. IR ($\nu(\text{CO})$)/(KBr-disk): 2046(s), 1996(vs), 1982(s), 1969(s), 1952(s) cm^{-1} for **1** and 2055(m), 2050(m, sh), 1993(s), 1969(vs), 1941(s) cm^{-1} for **2**. ^{31}P -NMR (CDCl_3): δ 57.8(s) and 68.8(s) for **1** and δ 55.9(d) ($J_{\text{P-H}} = 380$ Hz) and 71.2(s) for **2**. ^1H -NMR (CDCl_3): δ 4.15–4.29 (m, 18H) for **1** and 4.69(d) ($J_{\text{P-H}} = 380$ Hz) and 4.49–4.74 (m, 18H) for **2**.

Single crystals have not yet been obtained from the first main red band. This hampers the exact characterization of the main product.

X-ray Data Collection and Structure Determination

A dark green crystal of **1** with approximate dimensions of $0.55 \times 0.45 \times 0.20 \text{ mm}^3$ grown from hexane: CH_2Cl_2 was mounted on a MAC MXC³ diffractometer equipped with graphite monochromated MoK_α radiation ($\lambda = 0.71073 \text{ \AA}$). A dark green crystal of **2** (approximate dimensions of $0.40 \times 0.35 \times 0.10 \text{ mm}^3$) grown from hexane was mounted on the same diffractometer. Reflection data for both crystals were collected at room temperature (298 K). The crystal data for these compounds are given in Table I. The structure of **1** was solved by direct methods (SHELXS 86) and that of **2** was solved by MULTAN 78. Both structures were refined by a full-matrix least-squares method with a Crystan program package provided by MAC Science. Refinements were made anisotropically for nonhydrogen atoms for both compounds. The positions of the hydrogen atoms of the Cp rings in **1** were determined from the difference Fourier map and refined isotropically. Attempts were made to locate the positions of the H atoms of the Cp rings of **2** from the difference Fourier map; however, it was impossible to locate all the hydrogen atoms from the Fourier map. In addition, the function to locate the hydrogen atom at the calculated position is not included in the Crystan program package. The position of the H atom in the $\mu_2\text{-P(H)Fc}$ group of **2** is successfully determined from the difference Fourier map and refined isotropically. The molecular structures of **1** and **2** are displayed

TABLE I Crystal data

Compound	$\text{Co}_3(\text{CO})_7(\mu_3\text{-PFc})(\mu_2\text{-PFc}_2)$ (1)	$\text{Co}_3(\text{CO})_7(\mu_3\text{-PFc})(\mu_2\text{-P(H)Fc})$ (2)
Formula	$\text{C}_{37}\text{H}_{27}\text{Co}_3\text{Fe}_3\text{O}_7\text{P}_2$	$\text{C}_{27}\text{H}_{19}\text{Co}_3\text{Fe}_2\text{O}_7\text{P}_2$
Formula weight	989.9	805.8
Crystal system	Monoclinic	Monoclinic
Space group	$\text{P}2_1/n$	$\text{P}2_1/c$
a (Å)	16.043(4)	16.984(5)
b (Å)	18.174(3)	12.142(4)
c (Å)	12.562(2)	14.452(4)
β (deg)	91.45(2)	103.02(2)
V (Å ³)	3661(1)	2904(2)
Z	4	4
$d_{\text{calcd.}}$ /g cm ⁻³	1.80	1.84
Crystal dimensions (mm ³)	0.55 × 0.45 × 0.20	0.40 × 0.35 × 0.10
μ (MoK α) (cm ⁻¹)	15.0	15.7
Scan type	ω	ω
Scan range	1.35 + 0.35 tan θ	1.60 + 0.35 tan θ
Scan speed/deg min ⁻¹	5.0	5.0
$2\theta_{\text{max}}$ (deg)	50.0	55.0
Temperature (K)	298	298
Unique reflections	6441	5916
Reflections with $ F_o > 3\sigma(F_o)$	4387 ^a	4552
No. of parameters refined	556	382
R	0.055	0.060
R_w	0.075	0.072

MoK α radiation ($\lambda = 0.71073$ Å); $R = \sum ||F_o| - |F_c|| / \sum |F_o|$; $R_w = [\sum (|F_o| - |F_c|)^2 / \sum w(F_o)^2]^{1/2}$ where $w = 1/\sigma^2(F)$. ^a $|F_o| > 4\sigma(|F_o|)$.

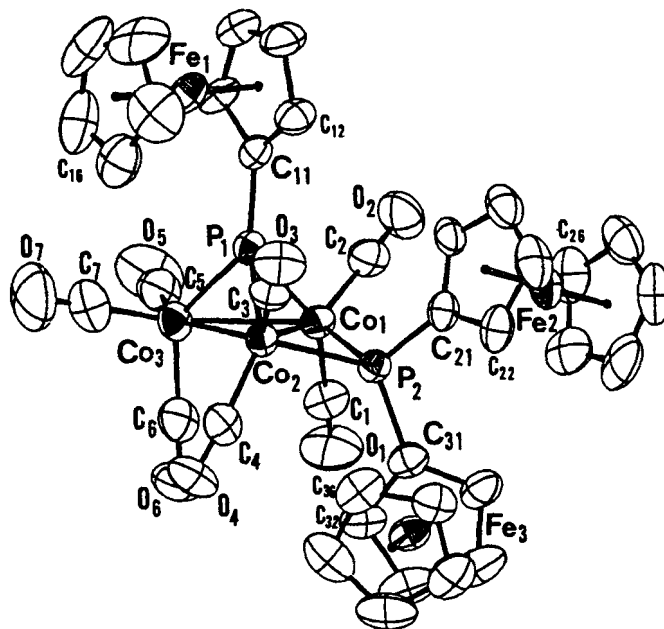


FIGURE 1 The molecular structure of $\text{Co}_3(\text{CO})_7(\mu_3\text{-PFc})(\mu_2\text{-PFc}_2)$ (1) together with numbering scheme.

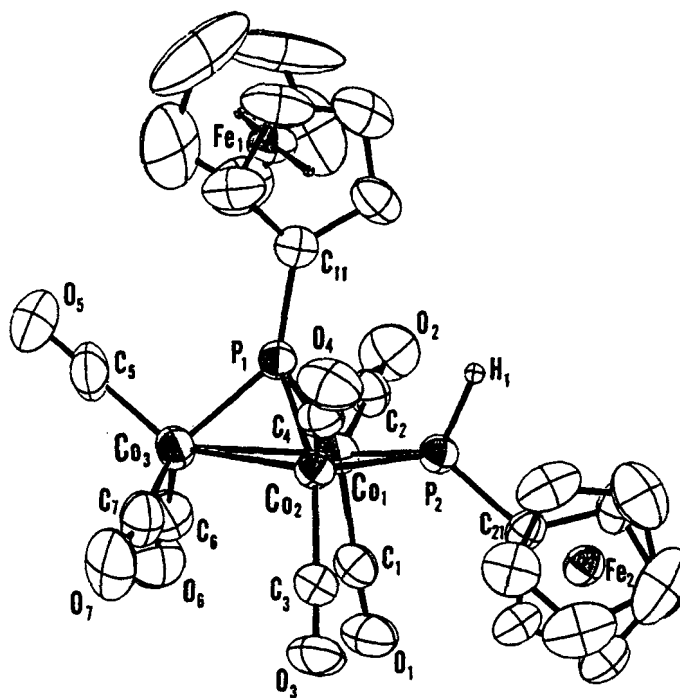


FIGURE 2 The molecular structure of $\text{Co}_3(\text{CO})_7(\mu_3\text{-PFc})(\mu_2\text{-P(H)Fc})$ (2) together with numbering scheme.

in Figures 1 and 2. The atomic coordinates are listed in Tables II and III and selected bond lengths and angles are given in Table IV. The $|F_o| - |F_c|$ tables and anisotropic temperature factor tables are available from S.O.

Electrochemical Measurements

Cyclic voltammetry was done at 25°C with a BAS CV-50W electrochemical analyzer equipped with a platinum electrode for the working electrode and a platinum coil for the auxiliary electrode. A Ag/AgNO_3 (0.01 M) electrode was employed as the reference electrode with 0.1 M $n\text{-Bu}_4\text{NClO}_4$ (TBAP) in CH_2Cl_2 . Approximately a 10^{-3} M solution was prepared in CH_2Cl_2 which contained 0.1 M TBAP as a supporting electrolyte. A sweep rate of 200 mV/s was generally used for CV. All of the manipulations were carried out under an argon atmosphere. The electrochemical data are tabulated in Table V and a typical cyclic voltammogram is shown in Figure 3.

TABLE II Atomic coordinates and isotropic thermal parameter, B_{eq} (\AA^2) of 1

Atom	x	y	z	B (eq)
Co1	0.26756 (7)	0.21998 (6)	0.05296 (8)	2.88 (4)
Co2	0.10974 (7)	0.21936 (6)	0.01562 (8)	2.81 (4)
Co3	0.21292 (8)	0.19350 (7)	-0.14351 (9)	3.54 (4)
Fe1	0.11867 (8)	0.44520 (8)	-0.1708 (1)	3.87 (4)
Fe2	0.22870 (8)	0.32322 (8)	0.3851 (1)	3.81 (4)
Fe3	0.05714 (8)	0.07638 (7)	0.3013 (1)	3.55 (4)
P1	0.1974 (1)	0.2917 (1)	-0.0527 (2)	2.93 (6)
P2	0.1711 (1)	0.2104 (1)	0.1727 (2)	2.70 (6)
C1	0.3210 (5)	0.1341 (6)	0.0762 (8)	4.1 (3)
C2	0.3451 (6)	0.2831 (6)	0.0875 (7)	4.1 (3)
C3	0.0294 (6)	0.2840 (5)	0.0336 (7)	3.7 (2)
C4	0.0569 (6)	0.1345 (6)	-0.0035 (8)	4.0 (3)
C5	0.3136 (8)	0.2015 (6)	-0.2006 (9)	5.5 (3)
C6	0.2095 (6)	0.0969 (6)	-0.1084 (8)	4.4 (3)
C7	0.1425 (8)	0.2012 (7)	-0.253 (1)	6.0 (4)
O1	0.3564 (5)	0.0816 (6)	0.0884 (4)	7.3 (3)
O2	0.3966 (5)	0.3249 (5)	0.1102 (6)	6.4 (2)
O3	-0.0209 (4)	0.3259 (4)	0.0494 (6)	5.7 (2)
O4	0.0216 (4)	0.0819 (4)	-0.0233 (6)	5.6 (2)
O5	0.3779 (6)	0.2027 (6)	-0.2355 (9)	9.0 (4)
O6	0.2111 (6)	0.0365 (4)	-0.0901 (7)	6.5 (3)
O7	0.0969 (7)	0.2044 (6)	-0.3251 (8)	10.3 (4)
C11	0.1993 (5)	0.3890 (5)	-0.0725 (6)	3.0 (2)
C12	0.1546 (6)	0.4437 (5)	-0.0144 (7)	3.7 (2)
C13	0.1725 (6)	0.5134 (6)	-0.0611 (9)	4.8 (3)
C14	0.2269 (6)	0.5028 (6)	-0.1425 (9)	4.4 (3)
C15	0.2436 (5)	0.4261 (5)	-0.1535 (7)	3.8 (2)
C16	0.0717 (9)	0.397 (1)	-0.308 (1)	7.1 (5)
C17	0.0236 (7)	0.3782 (9)	-0.227 (1)	5.9 (4)
C18	-0.0087 (8)	0.443 (1)	-0.180 (1)	7.7 (5)
C19	0.0214 (9)	0.5039 (9)	-0.234 (1)	7.6 (5)
C20	0.0727 (9)	0.476 (1)	-0.318 (1)	7.8 (5)
C21	0.1550 (5)	0.2865 (5)	0.2604 (6)	3.3 (2)
C22	0.1076 (6)	0.2929 (6)	0.3552 (7)	3.8 (2)
C23	0.1117 (7)	0.3689 (6)	0.3873 (9)	5.4 (3)
C24	0.1610 (7)	0.4078 (6)	0.3152 (9)	4.7 (3)
C25	0.1887 (6)	0.3578 (5)	0.2380 (6)	3.6 (2)
C26	0.3558 (6)	0.3174 (8)	0.386 (1)	5.6 (4)
C27	0.3296 (8)	0.3713 (7)	0.458 (1)	5.7 (4)
C28	0.2815 (9)	0.335 (1)	0.5339 (9)	6.5 (4)
C29	0.2773 (8)	0.2589 (9)	0.507 (1)	6.9 (4)
C30	0.3233 (7)	0.2474 (7)	0.414 (1)	5.4 (3)
C31	0.1616 (5)	0.1285 (5)	0.2516 (7)	3.3 (2)
C32	0.1554 (6)	0.0571 (5)	0.2041 (8)	4.1 (3)
C33	0.1553 (7)	0.0032 (7)	0.289 (1)	5.5 (4)
C34	0.1608 (6)	0.0417 (7)	0.385 (1)	5.7 (4)
C35	0.1654 (7)	0.1192 (6)	0.3655 (8)	4.6 (3)
C36	-0.0482 (6)	0.1264 (7)	0.2413 (9)	4.9 (3)
C37	-0.0504 (6)	0.0518 (7)	0.217 (1)	5.5 (3)
C38	-0.0461 (7)	0.0129 (6)	0.316 (1)	6.1 (4)
C39	-0.0428 (6)	0.0644 (6)	0.3986 (9)	5.1 (3)
C40	-0.0440 (6)	0.1330 (6)	0.3520 (8)	4.3 (3)
H12	0.108 (7)	0.441 (6)	0.036 (8)	3.69 (0)

TABLE II (Continued)

Atom	x	y	z	B (eq)
H13	0.160 (7)	0.560 (7)	-0.030 (9)	4.84 (0)
H14	0.248 (7)	0.529 (6)	-0.207 (9)	4.38 (0)
H15	0.270 (7)	0.390 (6)	-0.218 (9)	3.76 (0)
H16	0.089 (9)	0.374 (9)	-0.36 (1)	7.11 (0)
H17	0.020 (8)	0.327 (8)	-0.20 (1)	5.92 (0)
H18	-0.04 (1)	0.44 (1)	-0.13 (1)	7.71 (0)
H19	0.01 (1)	0.554 (9)	-0.24 (1)	7.66 (0)
H20	0.087 (9)	0.505 (8)	-0.38 (1)	7.81 (0)
H22	0.071 (7)	0.255 (6)	0.380 (8)	3.79 (0)
H23	0.088 (8)	0.392 (7)	0.45 (1)	5.38 (0)
H24	0.175 (7)	0.458 (7)	0.32 (1)	4.73 (0)
H25	0.228 (6)	0.370 (6)	0.167 (8)	3.59 (0)
H26	0.389 (8)	0.317 (7)	0.31 (1)	5.58 (0)
H27	0.337 (8)	0.423 (8)	0.45 (1)	5.75 (0)
H28	0.26 (1)	0.348 (9)	0.58 (1)	6.48 (0)
H29	0.243 (9)	0.216 (8)	0.55 (1)	6.90 (0)
H30	0.345 (8)	0.193 (7)	0.36 (1)	5.45 (0)
H32	0.136 (7)	0.039 (6)	0.122 (9)	4.08 (0)
H33	0.153 (8)	-0.056 (8)	0.27 (1)	5.52 (0)
H34	0.172 (7)	0.015 (7)	0.47 (1)	5.73 (0)
H35	0.167 (8)	0.150 (7)	0.41 (1)	4.57 (0)
H36	-0.046 (8)	0.162 (7)	0.20 (1)	4.89 (0)
H37	-0.041 (7)	0.012 (7)	0.15 (1)	5.50 (0)
H38	-0.047 (8)	-0.060 (7)	0.32 (1)	6.05 (0)
H39	-0.039 (8)	0.056 (7)	0.47 (1)	5.12 (0)
H40	-0.042 (7)	0.190 (6)	0.383 (8)	4.28 (0)

TABLE III Atomic coordinates and isotropic thermal parameter, B_{eq} (\AA^2) of 2

Atom	x	y	z	B (eq)
Co1	0.22512 (5)	0.11229 (7)	0.23369 (6)	3.09 (2)
Co2	0.21011 (5)	0.11034 (7)	0.40264 (6)	3.05 (3)
Co3	0.21636 (6)	0.30636 (7)	0.32080 (7)	3.47 (2)
Fe1	0.50422 (6)	0.22783 (9)	0.34533 (6)	3.55 (3)
Fe2	0.14726 (6)	-0.24975 (8)	0.39974 (6)	3.28 (3)
P1	0.3074 (1)	0.1850 (1)	0.3516 (1)	3.04 (4)
P2	0.2356 (1)	-0.0326 (1)	0.3242 (1)	3.02 (4)
C1	0.1228 (5)	0.0840 (6)	0.1660 (5)	3.6 (2)
C2	0.2834 (5)	0.0987 (6)	0.1481 (5)	4.0 (2)
C3	0.1044 (4)	0.0902 (6)	0.4043 (5)	3.5 (2)
C4	0.2599 (4)	0.0912 (6)	0.5219 (5)	3.9 (2)
C5	0.2786 (6)	0.4244 (7)	0.3401 (7)	5.6 (3)
C6	0.1522 (5)	0.3247 (7)	0.2048 (6)	4.9 (2)
C7	0.1486 (6)	0.3241 (6)	0.3980 (6)	5.1 (2)
O1	0.0604 (3)	0.0612 (5)	0.1270 (4)	5.3 (2)
O2	0.3218 (4)	0.0875 (5)	0.0937 (4)	6.4 (2)
O3	0.0394 (3)	0.0774 (5)	0.4090 (4)	5.7 (2)
O4	0.2922 (4)	0.0721 (6)	0.5978 (4)	6.2 (2)
O5	0.3199 (4)	0.4994 (5)	0.3526 (6)	8.4 (3)
O6	0.1109 (4)	0.3495 (6)	0.1351 (4)	6.9 (2)
O7	0.1050 (5)	0.3482 (5)	0.4436 (5)	8.4 (3)

TABLE III (Continued)

Atom	<i>x</i>	<i>y</i>	<i>z</i>	<i>B</i> (eq)
C11	0.4128 (4)	0.1707 (5)	0.4011 (4)	3.1 (2)
C12	0.4626 (5)	0.0803 (6)	0.3849 (6)	4.9 (2)
C13	0.5418 (5)	0.1024 (8)	0.4400 (7)	5.9 (3)
C14	0.5405 (5)	0.203 (1)	0.4882 (6)	5.9 (3)
C15	0.4604 (5)	0.2490 (8)	0.4652 (5)	5.3 (2)
C16	0.4608 (7)	0.285 (1)	0.2115 (7)	6.6 (3)
C17	0.518 (1)	0.206 (1)	0.2098 (7)	9.9 (5)
C18	0.5880 (8)	0.246 (2)	0.270 (1)	14.1 (9)
C19	0.579 (2)	0.341 (2)	0.309 (1)	13.7 (9)
C20	0.491 (1)	0.370 (1)	0.271 (1)	9.8 (6)
C21	0.1731 (4)	-0.1515 (5)	0.2966 (4)	3.3 (2)
C22	0.0865 (4)	-0.1547 (6)	0.2876 (5)	3.8 (2)
C23	0.0623 (5)	-0.2684 (7)	0.2732 (5)	4.4 (2)
C24	0.1325 (6)	-0.3331 (7)	0.2726 (5)	5.0 (2)
C25	0.2026 (5)	-0.2626 (6)	0.2892 (5)	4.2 (2)
C26	0.1387 (6)	-0.1796 (8)	0.5268 (5)	5.2 (3)
C27	0.0891 (6)	-0.273 (1)	0.5074 (6)	6.6 (3)
C28	0.1372 (9)	-0.3659 (8)	0.4989 (6)	7.0 (4)
C29	0.2185 (7)	-0.3289 (9)	0.5123 (6)	6.7 (3)
C30	0.2180 (6)	-0.2147 (9)	0.5301 (5)	5.5 (3)
H1	0.314 (6)	-0.071 (7)	0.353 (6)	5.32 (0)

TABLE IV Selected bond lengths (Å) and angles (deg)

Compound	$\text{Co}_3(\text{CO})_7(\mu_3\text{-PFc})(\mu_2\text{-PFc}_2)$ (1)	$\text{Co}_3(\text{CO})_7(\mu_3\text{-PFc})(\mu_2\text{-P(H)Fc})$ (2)
<i>Distance</i>		
Co1–Co2	2.564 (1)	2.511 (1)
Co1–Co3	2.642 (1)	2.691 (1)
Co2–Co3	2.670 (2)	2.670 (1)
P1–Co1	2.156 (2)	2.136 (2)
P1–Co2	2.123 (2)	2.155 (2)
P1–Co3	2.136 (2)	2.109 (2)
P2–Co1	2.193 (2)	2.175 (2)
P2–Co2	2.188 (2)	2.169 (2)
P1–C11	1.785 (8)	1.781 (6)
P2–C21	1.792 (8)	1.783 (7)
P2–C31	1.798 (8)	
Co1–C1	1.797 (9)	1.824 (7)
Co1–C2	1.747 (9)	1.756 (8)
Co2–C3	1.764 (9)	1.818 (8)
Co2–C4	1.774 (9)	1.755 (7)
Co3–C5	1.79 (1)	1.764 (9)
Co3–C6	1.81 (1)	1.796 (8)
Co3–C7	1.77 (1)	1.79 (1)
C1–O1	1.12 (1)	1.117 (9)
C2–O2	1.15 (1)	1.14 (1)
C3–O3	1.13 (1)	1.132 (9)
C4–O4	1.14 (1)	1.135 (9)

TABLE IV (Continued)

Compound	$\text{Co}_3(\text{CO})_7(\mu_3\text{-PFc})(\mu_2\text{-PFc}_2)$	$\text{Co}_3(\text{CO})_7(\mu_3\text{-PFc})(\mu_2\text{-P(H)Fc})$
	(1)	(2)
C5-O5	1.13 (1)	1.14 (1)
C6-O6	1.12 (1)	1.13 (1)
C7-O7	1.14 (2)	1.13 (1)
P2-H1		1.39 (9)
<i>Angle</i>		
Co1-Co2-Co3	60.60 (4)	62.49 (4)
Co2-Co3-Co1	67.72 (4)	55.86 (3)
Co3-Co1-Co2	61.68 (4)	61.65 (4)
P1-Co1-Co2	52.61 (6)	54.53 (6)
P1-Co1-Co3	51.68 (6)	50.21 (5)
P1-Co2-Co1	53.78 (6)	53.84 (5)
P1-Co2-Co3	51.40 (6)	50.46 (5)
P1-Co3-Co1	52.34 (6)	51.11 (5)
P1-Co3-Co2	50.97 (6)	52.00 (6)
P1-Co1-P2	95.93 (8)	84.52 (7)
P1-Co2-P2	97.04 (8)	84.22 (7)
Co1-Co2-P2	54.26 (6)	54.79 (5)
Co2-Co1-P2	54.08 (6)	54.58 (5)
Co3-Co2-P2	112.87 (6)	116.68 (6)
Co1-P1-Co2	73.61 (7)	71.63 (6)
Co1-P1-Co3	75.98 (8)	78.68 (6)
Co2-P1-Co3	77.62 (8)	77.54 (7)
Co1-P2-Co2	71.65 (7)	70.62 (6)
P1-Co1-C1	149.6 (3)	151.4 (2)
P1-Co1-C2	96.5 (3)	103.3 (2)
P1-Co2-C3	143.5 (3)	153.7 (2)
P1-Co2-C4	97.6 (3)	98.9 (3)
P1-Co3-C5	105.3 (4)	98.6 (3)
P1-Co3-C6	132.4 (3)	123.0 (3)
P1-Co3-C7	105.6 (4)	119.8 (2)
P2-Co1-C1	99.3 (3)	96.2 (2)
P2-Co1-C2	113.2 (3)	111.4 (2)
P2-Co2-C3	104.3 (3)	102.3 (2)
P2-Co2-C4	105.1 (3)	153.7 (2)
C1-Co1-C2	101.3 (4)	103.0 (3)
C3-Co2-C4	104.4 (4)	103.2 (3)
C5-Co3-C6	102.1 (5)	105.2 (4)
C5-Co3-C7	104.3 (5)	104.5 (4)
C6-Co3-C7	104.1 (5)	103.2 (4)

TABLE V Voltammetric data

Compound	Oxidation	Reduction
	$E_{1/2}^a$	$E_{1/2}^a$
$\text{Co}_3(\text{CO})_7(\mu_3\text{-PFc})(\mu_2\text{-PFc}_2)$ (1)	0.33	-1.15, -1.34
$\text{Co}_3(\text{CO})_7(\mu_3\text{-PFc})(\mu_2\text{-P(H)Fc})$ (2)	0.48	-1.07

^a $E_{1/2}$ = half-wave potential (V).

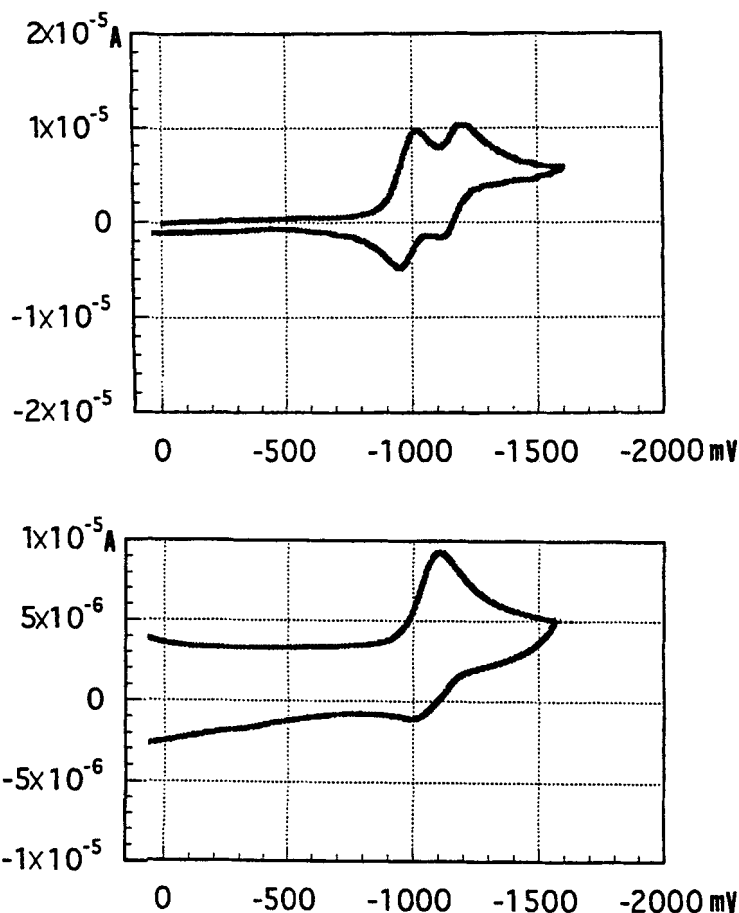


FIGURE 3 Cyclic voltammograms of $\text{Co}_3(\text{CO})_7(\mu_3\text{-PFc})(\mu_2\text{-PFc}_2)$ (1) (top) and $\text{Co}_3(\text{CO})_7(\mu_3\text{-PFc})(\mu_2\text{-P(H)Fc})$ (2) (bottom) in CH_2Cl_2 in the negative potential region at 25°C .

RESULTS AND DISCUSSION

We have attempted to improve the yield of 1 by employing high-purity AlCl_3 (99.9%) instead of standard-grade AlCl_3 (96%) in the procedure of the synthesis of FcPcCl_2 .² However, repeated trials have shown that neither 1 nor 2 were prepared when high-purity AlCl_3 was employed. The reason why 1 and/or 2 is not obtained when high-purity AlCl_3 is used for the synthesis of Fc_2PcCl is not clear at present.

The molecular structures of both compounds have been successfully solved and refined as described in the Experimental section. The position of

the H atom in the bridging μ_2 -P(H)Fc group of **2** has been determined from the difference Fourier map. Additional evidence for the existence of the H atom in this bridging group has been provided from ^1H and ^{31}P -NMR spectra as described in the Experimental section. The total skeletal electrons are 48 for both clusters. Sharp NMR signals (^1H and ^{31}P) and these electron counts suggest that both clusters are diamagnetic. The molecular structures of **1** and **2** are quite similar (Figures 1 and 2) with an apical μ_3 -bridging PFc group and a μ_2 -bridging P(R)Fc group. In **2** however, the bridging μ_2 -P(H)Fc group is significantly pulled-up toward the apical μ_3 -PFc group and the CO group in an equatorial position on the Co3 atom is lessened from two (cluster **1**) to one. This subtle change in the structure is confirmed by comparing the P1–Co1–P2 and P1–Co2–P2 bond angles for both clusters; P1–Co1–P2 and P2–Co2–P2 angles for **1** are $95.93(8)^\circ$ and $97.04(8)^\circ$, respectively while P1–Co1–P2 and P1–Co2–P2 angles for **2** are $84.52(7)^\circ$ and $84.22(7)^\circ$, respectively. The comparison of bond-lengths and angles for **1** and **2** from Table IV indicates that the distances between Co1 and Co2, which the μ_2 -P(R)Fc (R = H or Fc) bridges, are significantly shorter than the distances between Co1 and Co3 and between Co2 and Co3 for both clusters. This shortening is enhanced in **2**; $r(\text{Co1–Co2}) = 2.511(1)\text{ \AA}$ is 0.16 \AA shorter than $r(\text{Co1–Co3}) = 2.691(1)\text{ \AA}$ and $r(\text{Co2–Co3}) = 2.670(1)\text{ \AA}$, while $r(\text{Co1–Co2}) = 2.564(1)\text{ \AA}$ is 0.08 \AA shorter than $r(\text{Co1–Co3}) = 2.642(1)\text{ \AA}$ and $r(\text{Co2–Co3}) = 2.670(2)\text{ \AA}$ in **1**. Although these shortenings are significant for **1** and **2**, the distances are typical for a single Co–Co bond (2.52 \AA for $\text{Co}_2(\text{CO})_8$, 2.49 \AA for $\text{Co}_4(\text{CO})_{12}$, 2.47 \AA for $\text{CH}_3\text{CCO}_3(\text{CO})_9$, and 2.47 \AA for $\text{Cp}_4\text{Co}_4\text{H}_4$)³ and considerably longer than those of double Co=Co bonds (2.253 \AA for Cp_2^*Co_2 and $2.372(2)$ and $2.359(2)\text{ \AA}$ for $[\text{CpCo}(\text{CO})]_2^{2+}$).^{4,5} Thus it is anticipated that the bridging μ_2 -P(R)Fc group is responsible for the shortening of the Co1–Co2 bond lengths for both clusters. Next we are interested in the enhanced shortening of this bond in **2** and compare the P2–Co1 and P2–Co2 bond lengths for both clusters; the P2–Co1 and P2–Co2 bond lengths in **2** are approximately 0.02 \AA shorter than those in **1**. The comparison of the skeletal Cok–Col–Com (k, l, m = 1 or 2 or 3) angles affords another hint to interpret the result; Co2–Co3–Co1 for **2** is $55.86(3)^\circ$ and is the smallest in three Cok–Col–Com angles while this angle for **1** is $67.72(4)^\circ$ and is the largest in three Cok–Col–Com angles. The P(H)Fc group is less bulky than the PFc₂ group. Therefore, it is considered that the less bulky P(H)Fc group in **2** can approach closer to Co1 and Co2 than PFc₂ does in **1** and less bulkiness of the bridging μ_2 -P(H)Fc group is mainly responsible for this shortening of the Co1–Co2 bond length in **2**.

The most interesting characteristic for **1** and **2** is that both clusters have multiple ferrocenyl groups which are redox-active and therefore exploration of the redox chemistry by CV for both clusters is attractive. In the previous communication, we reported that only one peak assignable to the oxidation of the ferrocenyl groups is observed in the positive potential region for **1** at room temperature. This observation suggests that the oxidation potentials for ferrocenyl groups which are in different circumstances are similar and the three ferrocenyl groups do not interact electronically with each other. Although two ferrocenyl groups in **2** are under different surroundings than **1**, the cyclic voltammogram is similar to that of **1** in the positive potential region at room temperature. The cyclic voltammogram of **2** in the negative potential region, however, is different from that of **1** as shown in Figure 3; two reduction peaks are observed for **1** while only one reduction peak is observed for **2** at room temperature. These peaks are assigned to the reduction of the Co₃ core.^{6,7} The Co₃ core reduction takes place at one step for **2**. One plausible explanation for the occurrence of two reduction peaks in **1** is that the first reduction step occurs at Co1 and Co2 to which the PFC₂ group bridges and the second reduction occurs at Co3. In order to confirm this assignment, the measurement of the exact current at each reduction step is needed. However, it has been shown that the anion is unstable either for **1** or **2** at room temperature. Repeated potential sweeps in the negative potential region for both clusters diminish the peak intensity rapidly. This instability has hampered further exploration.

Acknowledgements

The present research was financially supported by Tokai Foundation for Technology and Iketani Science and Technology Foundation.

References

- [1] S. Onaka, H. Muto, Y. Katsukawa and S. Takagi, *J. Organomet. Chem.*, **543**, 241 (1997).
- [2] G.P. Sollott and W.R. Peterson Jr., *J. Organomet. Chem.*, **19**, 143 (1969).
- [3] H. Lorenz, *Chem. Ber.*, **108**, 973 (1976).
- [4] N.E. Schore, C.S. Ilenda and R.G. Bergman, *J. Am. Chem. Soc.*, **99**, 1781 (1977).
- [5] J.J. Schneider, R. Goddard, S. Werner and C. Krüger, *Angew. Chem. Int. Ed. Engl.*, **30**, 1124 (1991).
- [6] S. Onaka, M. Otsuka, S. Takagi and K. Sako, *J. Coord. Chem.*, **37**, 151 (1996); S. Onaka, Y. Katsukawa and H. Furuta, *J. Coord. Chem.*, **42**, 77 (1997).
- [7] S.B. Colbran, B.H. Robinson and J. Simpson, *Organometallics*, **2**, 943 (1983); **2**, 952 (1983); **3**, 1344 (1984).